

Electronic Supplementary Information (ESI)

Intrinsic formation of nanocrystalline neptunium dioxide in the neutral aqueous condition relevant to deep geological repositories

Richard Husar,^a René Hübner,^b Christoph Hennig,^{a,c} Philippe M. Martin,^d
Mélanie Chollet,^d Stephan Weiss,^a Thorsten Stumpf,^a
Harald Zänker,^a and Atsushi Ikeda-Ohno^{a*}

^a *Institute of Resource Ecology, Helmholtz-Zentrum Dresden-Rossendorf (HZDR)
Bautzner Landstrasse 400, D-01328 Dresden, Germany*

^b *Institute of Ion Beam Physics and Materials Research, Helmholtz-Zentrum Dresden-Rossendorf
(HZDR)
Bautzner Landstrasse 400, D-01328 Dresden, Germany*

^c *The Rossendorf Beamline (ROBL), European Synchrotron Radiation Facility (ESRF)
BP 220, F-38043 Grenoble, France*

^d *Commissariat à l'énergie atomique et aux énergies alternatives (CEA)
DEN, DEC, Cadarache, F-13108 Saint-Paul-Lez-Durance, France*

* E-mail: a.ikeda@hzdr.de, Tel: +49-351-260-3156

Contents

Experimental details	3
Preparation of Np(IV) solution and synthesis of nanocrystalline NpO ₂	3
X-ray absorption spectroscopy	3
Transmission electron microscopy	3
Sample appearance	4
X-ray absorption spectroscopy	4
XANES.....	4
EXAFS.....	5
Transmission electron microscopy	6
Energy-dispersive X-ray	6
TEM micrograph	7
References	7

Experimental details

Preparation of Np(IV) solution and synthesis of nanocrystalline NpO₂

The Np(IV) stock solution employed in this study ($[\text{Np}]_{\text{total}} = 56 \text{ mM}$ in 1 M HNO_3) was electrochemically prepared from the Np(V) solution, according to the procedure described previously.¹ The as-prepared Np(IV) stock solution was neutralised with sodium bicarbonate and filtrated with a 5 kDa membrane filter to obtain a colloid-free weakly basic solution of Np(IV) ($[\text{Np}]_{\text{total}} = 9.8 \text{ mM}$ in $1 \text{ M NaHCO}_3 / 1 \text{ M HNO}_3$ at $\text{pH} = 8.6$, Solution **1** in Figure 1). The solution was further diluted with a deoxygenated ultrapure water ($\text{pH} = 7.0$). The resultant solution with $[\text{Np}]_{\text{total}} = 1.0 \text{ mM}$ (Solution **2** in Figure 1) was left in an inert glove box for three hours to allow the sedimentation of a yellow-brownish precipitate. The precipitate was separated from the solution by centrifugation, washed with the ultrapure water three times, and redispersed in the ultrapure water (Solution **3** in Figure 1). All the processes were performed in the inert glove box and the precipitate was always kept wet. The Np concentrations were determined by liquid scintillation counting (Wallac 1414, Perkin Elmer,) and ICP-MS (Elan 9000, Perkin Elmer). UV/Vis absorption spectra were recorded on a TIDAS 100 spectrophotometer (J&M Analytik AG) with an acrylic/polystyrene cuvette (10 mm path length). Zeta potential measurements were performed with a Zetasizer Nano ZS (Malvern Instruments). All the UV/Vis absorption and zeta potential measurements were carried out in the inert glove box.

X-ray absorption spectroscopy

X-ray absorption spectra were collected in a fluorescence mode at the Rossendorf Beamline² at the European Synchrotron Radiation Facility. Aqueous samples were measured under ambient conditions, whilst powder and wet precipitate samples were measured at 15 K with a He cryostat. The wet precipitate sample was obtained by diluting Solution **1** with ultrapure water without further washing. The sample was sealed by hot melting and stored in anaerobic during transport and until measurement. A reference compound of NpO₂ powder was provided from CEA Cadarache. The lattice parameter obtained for this NpO₂ powder ($Fm\bar{3}m$, $5.434(1) \text{ \AA}$) was in agreement with the reported value for NpO₂.³ Energy calibration of the acquired spectra was performed at the Y K-edge of Y metal foil, the first inflection point of which was defined at 17038 eV. The spectra were treated according to a standard procedure⁴ using software WinXAS⁵ and EXAFSPAK⁶ using theoretical phase and amplitude functions calculated with the FEFF 8.20 code⁷ based on the crystal structure of $\text{Na}_6[\text{U}(\text{CO}_3)_5] \cdot 12\text{H}_2\text{O}$ ⁸ and NpO₂.³ For EXAFS curve fitting, the amplitude reduction factor, S_0^2 , was defined as 0.9, whilst the threshold energy, $E_{k=0}$, was defined at 17625 eV and varied as a global fit parameter.

Transmission electron microscopy

Samples for TEM measurements were prepared by dropping a drop of Solution **3** on a carbon-coated copper grid (400 mesh, S 160, Plano GmbH) and drying it under an inert atmosphere. Bright-field TEM images were collected on an image-corrected Titan 80-300 electron microscope (FEI) operating at 300 kV. Selected area electron diffraction (SAED) patterns were acquired from a specimen area of 190 nm in diameter. Energy-dispersive X-ray spectroscopy (EDXS) was performed in the scanning TEM mode with a Li-drifted silicon detector (EDAX).

Sample appearance

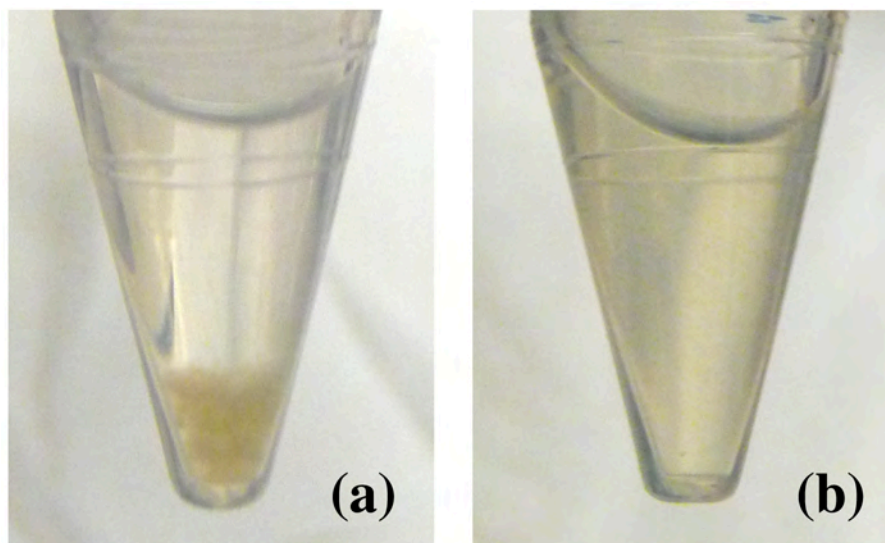


Figure S1. Appearance of Np(IV) solution in NaHCO_3 : (a) 24 hours after dilution with ultrapure water, showing yellow/brownish precipitate, (b) redispersion of the precipitate deposited in (a) into ultrapure water.

X-ray absorption spectroscopy

XANES

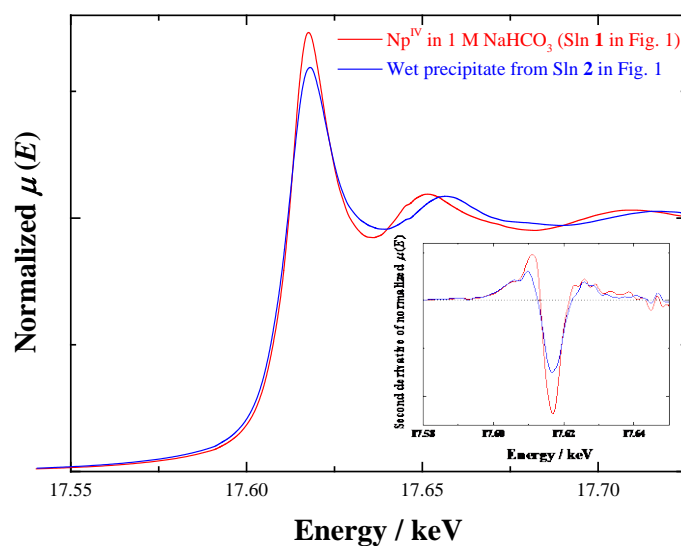


Figure S2. Np L_{III} -edge XANES spectra for Np(IV) in 1 M NaHCO_3 /1 M HNO_3 (Solution **1** in Figure 1 in the main text) and wet precipitate obtained from Solution **2** in the main text, and their corresponding second derivatives (inset).

Table S1. XANES edge positions at Np L_{III} -edge for the spectra given in Figure S2. The edge position is defined at the first inflection point

Sample	Edge position / keV
Np(IV) in 1 M NaHCO ₃ / 1 M HNO ₃	17.6134
Wet precipitate	17.6126

EXAFS

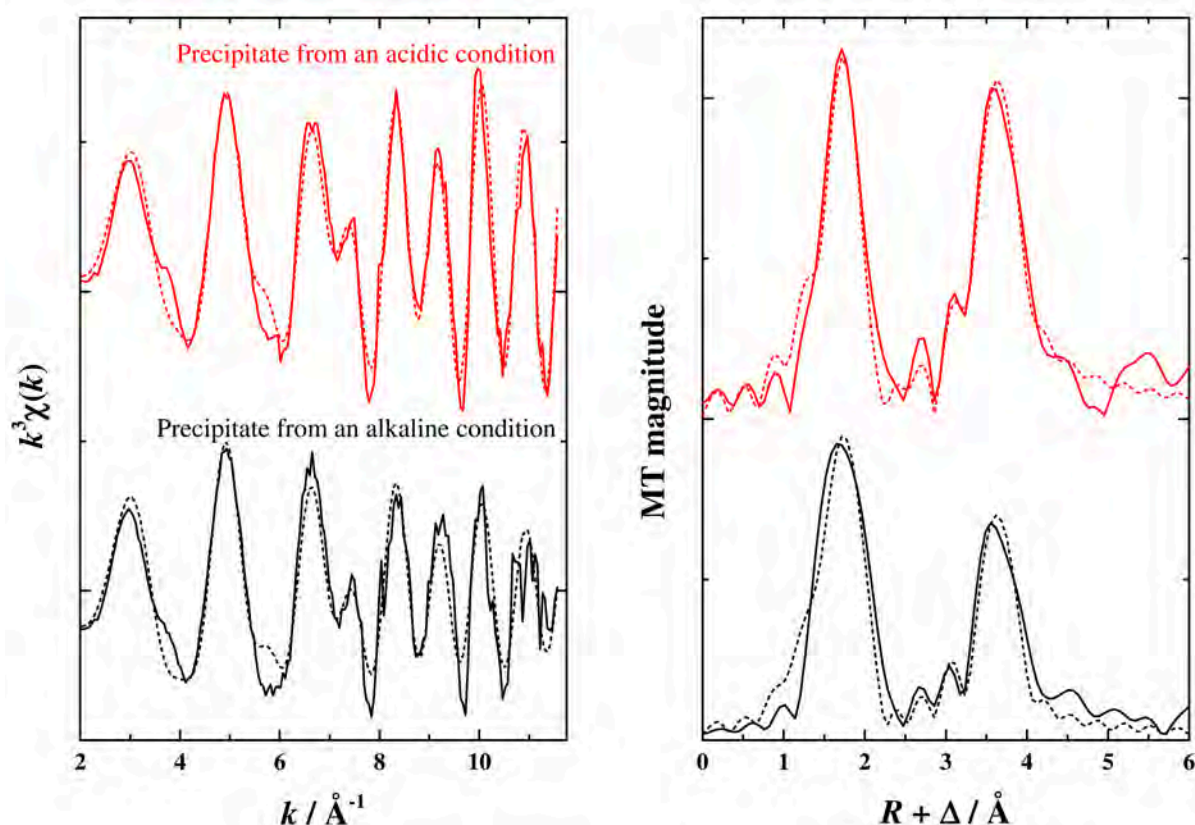


Figure S3. k^3 -weighted Np L_{III} -edge EXAFS spectra for Np(IV) precipitate obtained from acidic (red) and alkaline (black) conditions (left) and their corresponding Fourier transforms (FTs, right). Phase shifts (Δ) are not corrected on the FTs. The black-coloured data are identical to those for “Wet precipitate” in Fig. 2 in the main text, whilst the red-coloured data are identical to those for “NpOac” in Fig. 4 of reference [9], which was obtained by neutralising 0.01 M Np(IV) in 1 M HNO₃ with NaOH. The EXAFS spectrum for “Precipitate from an acidic condition” shows clearer oscillation pattern with larger amplitude than that for “Precipitate from an alkaline condition”. This is an indication that the former precipitate is more structurally ordered (i.e. less amorphous) than the latter precipitate. Hence, it is likely that the precipitate from the acidic condition contains less hydroxide amorphous phases than those from the alkaline condition.

Table S2. EXAFS structural parameters obtained from theoretical curve fitting

Sample	Scattering path	$R / \text{\AA}^a$	CN^b	$\sigma^2 / \text{\AA}^2$	$\Delta E_{k=0} / \text{eV}$	F-test
Np(IV) in 1 M NaHCO ₃ (solution 1)	Np-O(CO ₃)	2.44	10.2	0.0110	1.4	0.22
	Np-C(CO ₃)	2.86	5.1	0.0069		
	Np-O _{dist} (CO ₃)	4.18	4.8	0.0091		
	MS ^c (CO ₃)	4.18	4.8	0.0091		
Wet precipitate from solution 2	Np-O1	2.26	2.4	0.0071	-7.9	0.25
	Np-O2	2.39	3.6	0.0071		
	Np-Np	3.83	3.6	0.0052		
NpO ₂	Np-O	2.31	8.3	0.0043	0.4	0.76
	Np-Np	3.84	11.8	0.0013		
	Np-O _{dist}	4.47	25.3	0.0022		

^a Interatomic distance R , errors $\leq \pm 0.02 \text{ \AA}$, ^b Coordination number CN , errors $\leq \pm 15\%$, ^c MS; multiple scattering paths assuming the linear Np-C-O_{dist} arrangement.

Transmission electron microscopy

Energy-dispersive X-ray

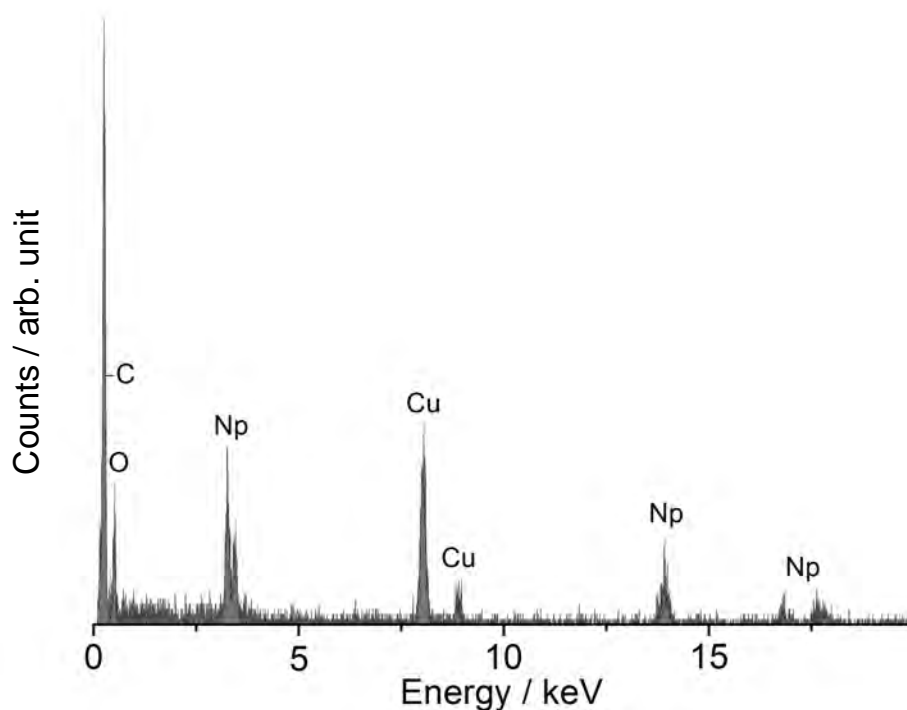


Figure S4. Energy-dispersive X-ray (EDX) spectrum of the dried precipitate obtained from Solution 3 (see Experimental details). The C and Cu signals are associated with a carbon-coated copper grid used for TEM measurement.

TEM micrograph

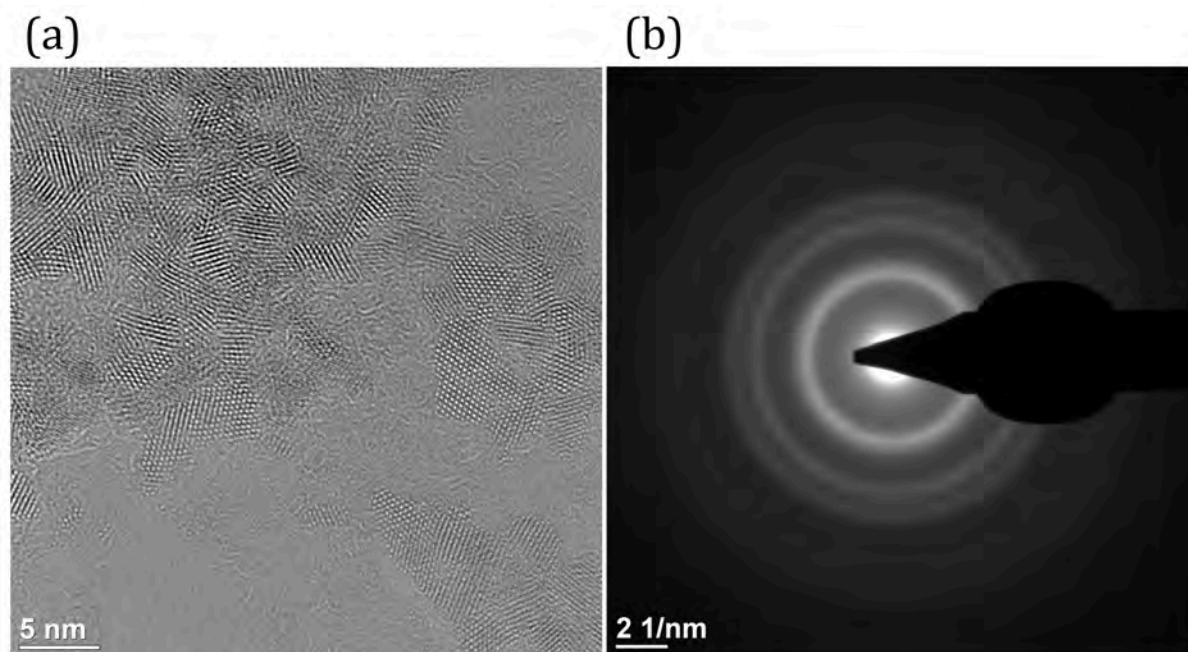


Figure S5. (a) HR-TEM image acquired for the precipitate obtained directly from Solution 2 without washing process and (b) corresponding selected area electron diffraction (SAED) pattern which is consistent with fluorite-type NpO_2 structure (ICSD card 647176).

References

- [1] A. Ikeda-Ohno, C. Hennig, A. Rossberg, H. Funke, A. C. Scheinost, G. Bernhard, T. Yaita, *Inorg. Chem.* **2008**, *47*, 8294-8305.
- [2] W. Matz, N. Schnell, G. Bernhard, F. Prokert, T. Reich, J. Claußner, W. Oehme, R. Schlenk, S. Dienel, H. Funke, F. Eichhorn, M. Betzl, D. Pröhl, U. Strauch, G. Hüttig, H. Krug, W. Neumann, V. Brendler, P. Reichel, M. A. Denecke, H. Nitsche, *J. Synchrotron Radiat.* **1999**, *6*, 1076-1085.
- [3] G. Lander, M. Mueller, *Phys. Rev. B* **1974**, *10*, 1994-2003.
- [4] D. C. Koningsberger, R. Prins, *X-ray absorption: Principles, applications, techniques of EXAFS, SEXAFS and XANES*, Wiley-Interscience, New York, USA, 1988.
- [5] T. Ressler, *J. Synchrotron Radiat.* **1998**, *5*, 118-122.
- [6] G. N. George, I. J. Pickering, *EXAFSPAK, a suite of computer programs for analysis of X-ray absorption spectra*, 2000.
- [7] A. L. Ankudinov, B. Ravel, J. J. Rehr, S. D. Conradson, *Phys. Rev. B* **1998**, *58*, 7565-7576.
- [8] C. Hennig, A. Ikeda-Ohno, F. Emmerling, W. Kraus, G. Bernhard, *Dalton Trans.* **2010**, *39*, 3744-3750.
- [9] R. Husar, S. Weiss, C. Hennig, R. Hübner, A. Ikeda-Ohno, H. Zänker, *Environ. Sci. Technol. published as ASAP* (December 2014), DOI: 10.1021/es503877b.